Cell migration into scaffolds under co-culture conditions in a microfluidic platform†

Seok Chung,[a] Ryo Sudo,[a] Peter J. Mack,[b] Chen-Rei Wan,[a] Vernella Vickerman[c] and Roger D. Kamm*[ab]

Received 6th May 2008, Accepted 25th September 2008
First published as an Advance Article on the web 31st October 2008
DOI: 10.1039/b807585a

Capillary morphogenesis is a complex cellular process that occurs in response to external stimuli. A number of assays have been used to study critical regulators of the process, but those assays are typically limited by the inability to control biochemical gradients and to obtain images on the single cell level. We have recently developed a new microfluidic platform that has the capability to control the biochemical and biomechanical forces within a three dimensional scaffold coupled with accessible image acquisition. Here, the developed platform is used to evaluate and quantify capillary growth and endothelial cell migration from an intact cell monolayer. We also evaluate the endothelial cell response when placed in co-culture with physiologically relevant cell types, including cancer cells and smooth muscle cells. This resulted in the following observations: cancer cells can either attract (MTLn3 cancer cell line) endothelial cells and induce capillary formation or have minimal effect (U87MG cancer cell line) while smooth muscle cells (10T 1/2) suppress endothelial activity. Results presented demonstrate the capabilities of this platform to study cellular morphogenesis both qualitatively and quantitatively while having the advantage of enhanced imaging and internal biological controls. Finally, the platform has numerous applications in the study of angiogenesis, or migration of other cell types including tumor cells, into a three-dimensional scaffold or across an endothelial layer under precisely controlled conditions of mechanical, biochemical and co-culture environments.

Introduction

Cell migration is essential for a variety of physiological and pathological processes, such as angiogenesis, cancer metastasis, wound healing and inflammation. In the vascular system, significant efforts have focused on cell migration in the context of capillary morphogenesis. Through these studies, various mechanical and biochemical factors have been identified as critical in regulating endothelial cell migration and tube formation, such as chemotactic or chemokinetic effects of single and/or multiple growth factors,[1] interstitial fluid flow[2] and matrix stiffness.[3–5] Despite the detailed understanding of individual components, how these factors are integrated to produce a specific cellular response has yet to be elucidated, creating the need for a versatile *in vitro* system in which these environmental factors can be studied in a controlled fashion. Achieving this will facilitate investigations that lead to a better understanding of how biochemical and mechanical factors act together in physiological and patho-physiological processes and ultimately contribute to improved tissue engineering and therapeutic strategies.

Understanding cell migration in capillary morphogenesis is therapeutically important because of its relation to human diseases and developmental phenomena.[6] Typical cell migration assays are unable to integrate complex environmental factors, particularly those that facilitate the formation of new tube-like structures within a three dimensional environment from preformed capillaries or a cell monolayer. One of the current capillary morphogenesis assays produces planar tubular networks on ECM-like substrates.[7–9] Capillary-like structures formed with this technique, however, have a reversed cell polarity with media on the outside and scaffold materials on the inside.[7] Other approaches include sandwiching one cell monolayer between two layers of scaffold material[3,8] and inducing capillary invasion by introducing chemical gradients.[9] These experiments have provided a foundation for understanding certain aspects of capillary morphogenesis, but are limited by an inability to image cell invasion in-plane, which would lead to more detailed characterization of the factors influencing this biological process.

Historically, many assays have been used to study cell migration,[10] such as the wound assay,[11,12] the Teflon fence assay[13] and the Boyden chamber.[14,15] Both the wound assay and Teflon fence assay are limited to studying cell migration in 2D. The 2D research efforts are described in review references[3,10] and have provided new insights into the cellular and molecular mechanisms of cell migration. However, there remains a need for quantitative cell migration assays and 3D models that better mimic the physiologically relevant microenvironment of living

[a]*Department of Mechanical Engineering and Department of Biological Engineering, Massachusetts Institute of Technology, Cambridge, MA, USA. E-mail: rdkamm@mit.edu; Fax: +1-617-258-8559; Tel: +1-617-253-5330*
[b]*Harvard-MIT Division of Health Sciences and Technology, Massachusetts Institute of Technology, Cambridge, MA, USA*
[c]*Department of Chemical Engineering, Massachusetts Institute of Technology, Cambridge, MA, USA*
† Electronic supplementary information (ESI) available: Supplementary Fig. 1–6 and movie. See DOI: 10.1039/b807585a

tissues *in vivo* compared to previous 2D culture models.[16] The Boyden chamber is commonly used to study 3D migration, but is not conducive to quantifying cell migration in real time. Recently, a new assay with endothelial cell coated beads or spheroids embedded in collagen gel was used to generate tube-like structures in a three dimensional environment. The assay allowed the generation of stable tube-like structures,[17–19] but the initial endothelial cell seeding surface is a rigid bead that does not mimic certain physiological factors known to be important, such as the presence of a fluid-matrix interface with fluid shear stress and transendothelial flows. Furthermore, with the current assays, the chemokinetic and chemotactic effects are difficult to differentiate. Key challenges to the existing techniques are; (i) to have precise control of the mechanical and biochemical factors in a physiologically-relevant condition, (ii) to have excellent optical resolution in real time, and (iii) to minimize sample variability and enhance sensitivity for quantification.

Microfabrication and microfluidic technology has the potential to overcome these challenges by allowing for precise, simultaneous control of multiple environmental factors. However, efforts to-date in this area have continued to investigate one factor at a time. One example of this is microfabricated patterns, which have been used to demonstrate preferential cell migration in the direction of higher substrate stiffness.[20,21] Other microfabricated devices have also been developed to induce and monitor cell migration in the channel in response to either biochemical gradients or biomechanical forces.[22–26] These methods have also been used to apply well defined biochemical gradients to cells plated on the walls of a microfluidic channel,[22,23] or within gel scaffolds,[27,28] and demonstrate the potential to be a versatile tool for analyzing cellular responses under biochemical gradients. The need still exists, however, for a system that replicates a realistic 3D environment in combination with gradient and flow control to study cell migration and capillary morphogenesis. To satisfy these needs, microfluidic platforms have recently been developed, both by our laboratory integrating a hydrogel scaffold into a PDMS device for cell growth[29] and by others, in a device completely fabricated from hydrogel.[30,31] However, the capabilities of this approach in co-culture conditions to study tumor cell-induced angiogenesis or perivascular-endothelial cell communication and interaction and quantification of cellular morphogenesis have yet to be demonstrated.

Here, we present an advanced microfluidic approach to study cellular responses in 3D microenvironments. The new devices contain three independent flow channels with each channel separated by a 3D collagen scaffold filled through other microchannels. Endothelial cells can be grown in the center flow channel and a stimulus applied to one of the outside flow channels (*e.g.*, soluble factor or second cell type). With this configuration, the opposite outside channel serves as an internal control. In order to demonstrate the capabilities of this system as a migration assay, endothelial cell migration into the scaffold is monitored and quantified over time in response to multiple biophysical, biochemical or co-culture conditions, including scaffold stiffness, vascular endothelial growth factor (VEGF) gradients, and cell types (tumor cells or smooth muscle cells).

Experimental

PDMS microfluidic assay preparation

The microfluidic system is made of PDMS (poly-dimethyl siloxane, Silgard 184, Dow Chemical, MI, USA) using soft lithography with SU-8 (MicroChem, MA, USA) patterned wafers. The cured PDMS is removed from the wafer, trimmed and punched to form inlets and outlets. Both the fabricated PDMS device and glass coverslide are autoclaved and dried at 80 °C overnight. They are then plasma treated (PDC-001, Harrick, CA, USA) in air, and bonded together to form a closed microfluidic channel.

Collagen coating solution (50 μg/ml type I collagen; BD Biosciences, MA, USA) was introduced to the channels to facilitate cell adhesion. The device was then aspirated, washed with sterile water, and dried at 80 °C for 24 h, to render the hydrophilic channel surface hydrophobic (Fig. 1(a)). The hydrophilicity was made by plasma treatment for bonding. It should be rendered hydrophobic to confine the filled gel within the specified region. Posts in the gel region are also designed to help confine the scaffold material by surface tension.

Scaffold material was then introduced to the gel regions to form a gel scaffold. In these experiments, type I collagen (BD Biosciences, MA, USA) was used as a scaffold material and gelled in an incubator for 30 min at 37 °C (Fig. 1(b)). Gel stiffness was varied by adjusting the pH of pre-polymerized collagen solutions ranging from 7.4 to 11: the relaxation modulus of collagen polymerized at pH 11 is twice that at pH 7.4.[5] Following gelation, cell culture medium was then introduced to all microfluidic channels and the device was placed in an incubator (37 °C) for cell seeding (Fig. 1(c)).

Confirmation of chemical gradient

To confirm diffusion of biochemical factors, Texas Red-conjugated dextran (40 kDa; Invitrogen, CA, USA) was added to endothelial growth medium to a final concentration of 0.5 μg/ml and added to the condition channel to simulate recombinant human vascular endothelial growth factor (VEGF, 38.2 kDa; R&D Systems, MN, USA), a known stimulant of endothelial cell migration.[32,33] The experiments were conducted without cells. Diffusion profile was observed by fluorescence microscopy (Nikon, Tokyo, Japan) and intensity was measured by MATLAB. The distance in gel region was normalized by the length of the gel region. The intensity was normalized to 1 at the center of the condition channel.

Endothelial cell migration into collagen scaffolds under a gradient of growth factor

Human dermal microvascular endothelial cells (HMVEC) were commercially obtained (Lonza, NJ, USA) and cultured with endothelial growth medium (EGM-2MV; Lonza, NJ, USA) on regular culture flasks pre-coated with type I collagen for no more than 9 passages. Cell suspension was prepared with 2×10^6 cells/ml and filled into the central cell channel (Fig. 1(d)). After filling, the device was kept in the incubator at 37 °C for 30 min to allow cells to settle and attach to the substrate before the medium was replaced. VEGF-supplemented (20 ng/ml) medium was

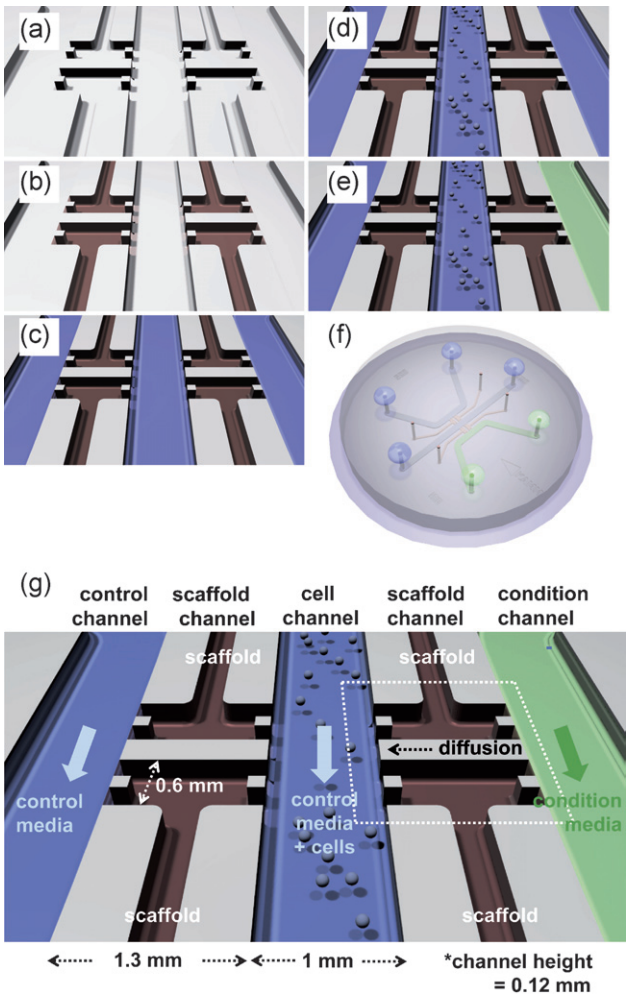

Fig. 1 Experimental protocol for the microfluidic assay development. (a) Prepared PDMS device made by soft lithography and surface treatment, (b) filled gel scaffold (indicated in brown) in the scaffold channel between the channels, (c) media (blue) filling both channels, (d) cell seeding (spheres) in the central cell channel, (e) chemical factors (green) applied in the condition channel. (f) Microfluidic device after filling of medium and chemical factors. Droplets are placed on all inlet ports to avoid evaporation of medium from the channels. Medium can be replaced with capillary forces generated by simply aspirating the existing droplets and adding new ones. (g) Schematic for microfluidic cell migration assay enabling direct comparison of cell migration behavior between the condition and control sides.

introduced into the condition channel to generate a gradient (Fig. 1(e, g)). 'VEGF at day N' means VEGF was applied N days after HMVEC seeding until the last day of cell tracking. In order to minimize evaporation from the channels and maintain zero flow conditions throughout the course of the experiment, 40 μl of medium is maintained as droplets at the inlets and outlets (Fig. 1(f)). Changing the media is accomplished by aspirating the existing droplet of medium and adding a new one on one side, using surface tension to drive flow due to the droplet size difference[34] to replenish media.

Cell migration was monitored by phase-contrast microscopy keeping the device in an incubator containing 5% CO_2 at 37 °C. All media were changed daily. Boundary perimeter of the monolayer and projected area of regions containing migrated cells were measured by ImageJ (http://rsbweb.nih.gov/ij/). The cell boundary was tracked manually. Immunofluorescence staining was performed to visualize the final cell distribution. Cells were fixed with 4% paraformaldehyde (Sigma-Aldrich, St. Louis, MO, USA) for 15 min at room temperature, and permeabilized with 0.1% Triton X-100 (Sigma-Aldrich) for 5 min. Actin filaments and nuclei were then stained with Rhodamine-Phalloidin (Sigma-Aldrich) and DAPI (Sigma-Aldrich), respectively. Fluorescent images were obtained using a phase-contrast microscope equipped with a fluorescent attachment (Nikon, Tokyo, Japan).

Endothelial cell migration into collagen scaffold under various co-culture conditions

1. MTLn3/U87MG and HMVEC co-culture. GFP-expressing rat mammary adenocarcinoma cells (MTLn3) were grown in α-minimum essential medium (α-MEM; Invitrogen, CA, USA) supplemented with 5% fetal bovine serum (FBS; Hyclone, UT, USA), 1mM $Na(HCO_3)_2$, 4 mM L-glutamin, 100 U/ml penicillin and 100 μg/ml streptomycin. GFP-expressing human glioblastoma cell line (U87MG) were grown in Dulbecco's modified Eagle medium (DMEM; Invitrogen, CA, USA) supplemented with 10% FBS, 1mM $Na(HCO_3)_2$, 4 mM L-glutamin, 100 U/ml penicillin and 100 μg/ml streptomycin. The U87MG cell suspensions were prepared at a concentration of 1×10^6 cells/ml and introduced to the condition channel. After filling, the device was kept in an incubator at 37 °C for 4 h to allow cells to settle and attach to the substrate before the medium was replaced. MTLn3 cell suspensions at concentrations of 1×10^6 cells/ml for high density and 0.5×10^6 cells/ml for low density were used, and were also introduced to the condition channel of other devices. After filling, the device was kept in the incubator at 37 °C for 4 h to allow cells to settle and attach to the substrate before the medium was replaced. The HMVEC suspension was prepared at 2×10^6 cells/ml as described above, and introduced to the central cell channel 1 day after MTLn3 or U87MG cell seeding. The cell channel was filled with endothelial growth medium and control/condition channels were filled with MTLn3 or U87MG growth medium as described above. Medium was changed daily. At the end of the experiment, cells were fixed and stained for actin and nuclei. GFP expression in MTLn3 and U87MG cell lines was detected to differentiate them from HMVEC.

2. HMVEC and 10T 1/2 co-culture. Mouse smooth muscle precursor cells (10T 1/2) were grown in HMVEC medium as described above and a suspension was prepared at 0.5×10^6 cells/ml. The suspension was introduced to the condition channel 1 day before HMVEC seeding into the center cell channel. After filling, the device was kept in the incubator at 37 °C for 30 min to allow cells to settle and attach to the substrate before the medium was replaced. Medium was changed daily. Double immunofluorescence staining was performed to distinguish HMVEC from 10T 1/2 in co-culture. After cells were fixed and permealilized as described above, they were sequentially incubated with Block Ace (Dainippon Phamaceutical, Osaka, Japan) for 1 h, and rabbit anti-von Willebrand factor antibody (Sigma-Aldrich) to label endothelial

cell cytoplasm. The cells were then rinsed with PBS, and incubated again with Alexa Fluor 488-conjugated anti-rabbit IgG antibodies (Invitrogen, Carlsbad, CA, USA). The cells were also stained for actin and nuclei as described.

Results and discussion

Cells were seeded and cultured in the center microfluidic channel (cell channel), in direct contact with the collagen scaffolds on either side. Cells migrated toward the two outside channels through the scaffold under the influence of biochemical and mechanical factors. The three channel design has a unique feature that allows the control and condition experiments to be performed simultaneously in the same device. One of the outside channels ("condition channel") contained the test agent while the other ("control channel") contained the control medium. Cell migration toward the condition channel or the control channel can thus be directly compared (Fig. 1(g)).

Quantification of concentration gradients

Biochemical diffusion and gradient generation were evaluated in the absence of cells using 40 kDa Texas Red-conjugated dextran. The dextran applied to the condition channel diffused toward the center channel eventually attaining a stable concentration gradient. Dextran first reached the center cell channel after about 30 min. The gradient then stabilized to a nearly linear concentration profile (5h) that was maintained at least 10 h (Supplementary Fig. 1(a)).† Intensity in the cell channel slowly increased about 10% in 10 h. In practice, the gradient could be maintained for over 24 h[28] and media replacement once a day can be used to replenish it.

It was interesting to observe the effect of the HMVEC monolayer on the chemical gradient. The HMVEC monolayer acted as an effective barrier to diffusion (Supplementary Fig. 1(b)),† and consequently, a sudden and steep gradient in concentration was formed at the monolayer. The steep gradient was also maintained at least 10 h. This situation is similar to what is likely to occur *in vivo* near existing capillaries completely closed by an endothelial cell monolayer.[42] The existence of such an abrupt change in concentration of a growth factor, for example, could result in differences in cell polarity on the condition and control sides of the central channel monolayer. The cell monolayer on the condition side receives growth factors *via* the scaffold (basal membrane), while that on the control side receives growth factors from medium in the channel (apical membrane). The cell polarity difference likely contributed to the dramatic responses of HMVEC (Fig. 2 and 4). The accumulation with minimized leak also suggests that the HMVEC monolayer is complete and intact.

Quantified endothelial cell migration

Perimeter and area changes of migrating cells into soft (pH 7.4) and rigid (pH. 11.0) scaffolds were studied. Collagen scaffolds were monitored and quantified over several days under a VEGF gradient originating from the condition channel (Fig. 2(a)). Cells rapidly migrated into the scaffold between the center and condition channels, while significantly less migration was observed on the control side (Fig. 2(b) and (c)).

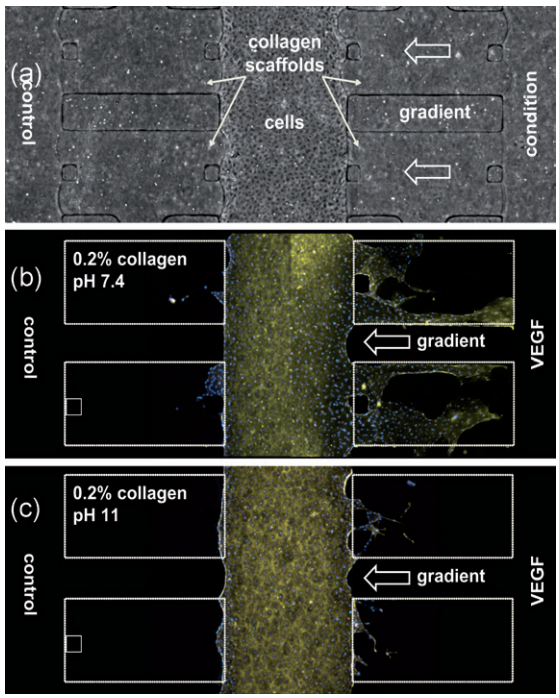

Fig. 2 Growth factor-induced endothelial cell migration. (a) One day after HMVEC seeding a confluent monolayer was formed in the cell channel and growth factor (20 ng/ml of VEGF) was then applied in the condition channel. (b) Migration results of HMVEC into 0.2% (2 mg/ml) collagen gel scaffold polymerized at pH, 7.4 and (c) at pH 11.0. Cells were fixed after 6 days of culture with 5 days of VEGF gradient application, and stained for actin by Rhodamine-phalloidin (yellow) and nuclei by DAPI (blue). White dotted lines indicate the outlines of gel scaffold and small rectangles in the scaffold region indicate the PDMS posts of 150 μm × 150 μm. Cells preferentially migrated into the gel on the condition side up the VEGF gradient.

Supplementary Fig. 2† shows the method used to quantify the perimeter and area of cell migration. To examine the time-dependence of this process, VEGF was applied to the condition channel 1, 2 or 3 days after cell seeding. Results are presented in two ways: the normalized values and the relative normalized values. For the normalized values, the measured data were normalized to their own baseline data at the initial time point:

$$[F_n] = \frac{F_n - F_0}{F_B} \quad (1)$$

where "F" represents either the length of the outer perimeter (L) or the projected area (S) of the capillary structures (see Supplementary Fig. 2).† Subscripts denote either the initial value (F_0), the baseline value (F_B) or the value at time point n (F_n).

Relative normalized values were assessed as the difference between the normalized values on the condition side (cond) and the control side (contr):

$$[F_n]_{\text{relative}} = [F_n]_{\text{cond}} - [F_n]_{\text{contr}} \quad (2)$$

When plotting the normalized values, no significant trends were observed (see comparison in Supplementary Fig. 3).† However, when we plotted the relative normalized values on the ordinate, significant trends in the length and area of cell migration for different durations of VEGF application (Fig. 3(a) to (d)) were observed.

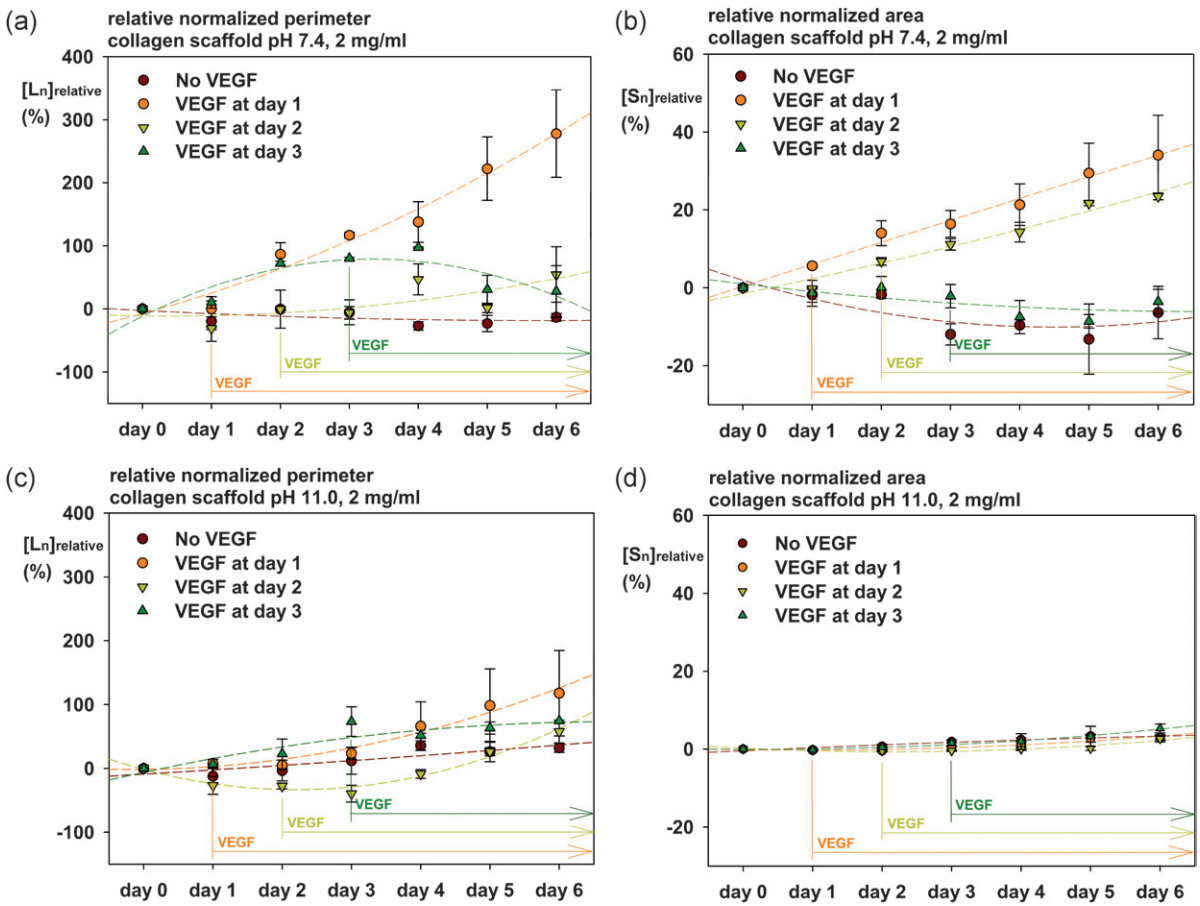

Fig. 3 (a) Graph of normalized relative perimeter of migrated cells in the 0.2% (2.0 mg/ml) collagen gel scaffold polymerized at pH 7.4. 'No VEGF' serves as the negative control without VEGF gradient. 'VEGF at day *n*' means that VEGF was first applied *n* days after cell seeding and continued to the end of the experiment. (b) Graph of normalized relative area of migrated cells in the collagen gel scaffold. (c and d) Graphs of normalized relative perimeter and area of migrated cells in the collagen gel scaffold. Each point represents an average with $n = 8$ (8 scaffolds; 4 devices) for each condition. Error bars represent standard deviation.

In Fig. 3(a), (b) and (c), graphs of 'VEGF at day 1' increased while other graphs of 'VEGF at day 3' and 'no VEGF' decreased or were flat. The graphs of 'VEGF at day 2' showed an increase in Fig. 3(b), but exhibited less of an effect in other figures. The increase means that cell migration into the scaffold continues increasing on the condition side, while that into the control side is stable or regresses. Slopes of relative normalized perimeter and area demonstrate that, with collagen gel polymerized at pH 7.4 or 11.0, VEGF added 1 day after cell seeding apparently induced cell migration, while VEGF added after 3 days did not. VEGF added 2 days after cell seeding could be considered to induce cell migration (Fig. 3(b)), but not as strongly as VEGF added 1 day after cell seeding. Changes in the relative normalized values of the area change were, however, too small to be detected in the collagen scaffolds polymerized at pH 11.0 (Fig. 3(d)). Relative normalized values provide insights that are not apparent when studying normalized values alone. High sensitivity could be achieved by comparing the condition and control sides in the same device, eliminating chip-to-chip variability.

The different responses of the HMVECs to time-dependent VEGF presentation can be explained by differences in cell confluence in the cell channel. HMVEC seeding density in the experiments was fixed (2×10^6 cells/ml). This density always formed a confluent monolayer 1 or 2 days after cell seeding. Without VEGF, cells in the monolayer were relatively stable. Some cells migrated into the scaffold, but regressed in 3 or 4 days. The receding or flat slope shows this situation. When VEGF was applied 1 or 2 days after cell seeding, the cells in the monolayer responded to VEGF and the slope kept increasing until the last day of experiments. However, when VEGF was applied 3 days after cell seeding, the cells in the monolayer were overconfluent and responded less, leaving the slope decreasing or flat. This suggests that VEGF applied 3 days after cell seeding does not attract the cells to migrate into the scaffold. It is consistent with the concept that the cells in a confluent monolayer become less responsive to additional growth factors and further growth is limited by contact inhibition.[35]

The influence of the mechanical properties of collagen scaffold on angiogenesis

The observed endothelial cell migration patterns demonstrated here depended on collagen gel stiffness (Fig. 2(b) and (c)). As discussed above, gel stiffness can be controlled by adjusting the initial pH of the collagen solution before polymerization with

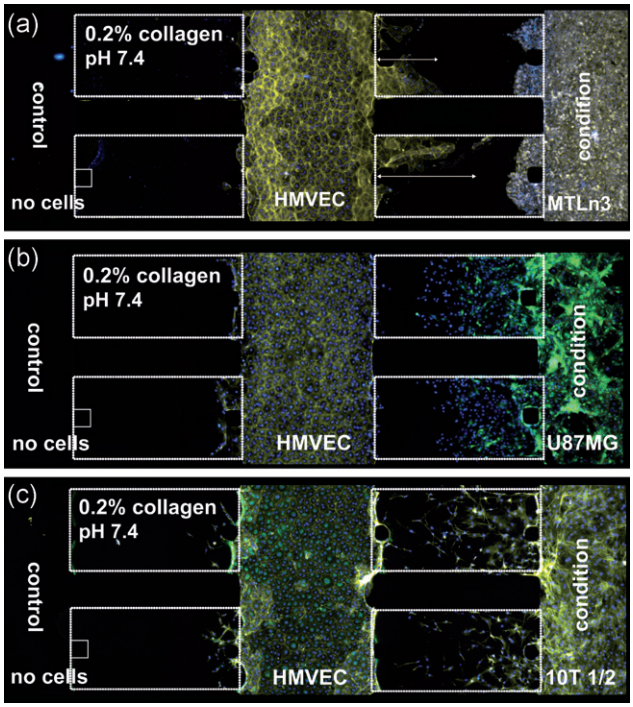

Fig. 4 Proof-of-principle utility of the microfluidic cell migration platform with other cell types and in co-culture. Cells were fixed and stained for actin by Rhodamin-Phalloidin (yellow) and for nuclei with DAPI (blue). Concentration and pH at polymerization of collagen gel are indicated in the corner of scaffold region. 0.2% means collagen concentration of 2.0 mg/ml. White dotted lines delineate the collagen gel scaffold while the small white rectangle marks a PDMS post (150 μm × 150 μm). (a) Co-culture of HMVEC and MTLn3 (seeded at ~1,000 cells/mm^2). 4 days after HMVEC seeding and 5 days after MTLn3 seeding. Migration of HMVEC is faster on the condition side than the control side. (b) Co-culture of HMVEC and U87MG cells. 7 days after HMVEC seeding and 8 days after U87MG seeding. U87MG express GFP (green) which can be used to distinguish the cells from HMVEC. Note similar migration characteristics on the condition and control sides. (c) Co-culture of HMVEC and 10T 1/2. 4 days after HMVEC seeding and 5 days after 10T 1/2 seeding. HMVEC were stained for von Willebrand factor (green) to distinguish them from 10T 1/2. Note HMVEC migration only on the control side.

higher pH values resulting in stiffer gels.[5] Comparing endothelial sprouting in gels prepared at pH 7.4 and pH 11 revealed that stiffer collagen gels (polymerized at pH 11) restrict endothelial cell migration, but promote the generation of tube-like structures (Supplementary Fig. 4(a))† with diameters in the range of 20–30 μm. Formed structures resemble tube-like capillaries observed in other assays.[9,19] The existence of a lumen was subsequently confirmed by introducing 2 μm-diameter microbeads into the culture medium and tracking microbead motion using fluorescence microscopy (Supplementary Fig. 4(b)–(d)).† Flow was produced in this instance by increasing fluid pressure in the central cell channel above that in the condition channel by controlling the droplet size, and therefore, the relative pressures generated by capillarity forces.[34] Time-lapse particle tracking of microbeads was performed demonstrating that the beads flowed only within the tube-like structure accumulating at the end of the capillary structures over time.

The role of gel stiffness on the structure of migrated endothelial cells can also be illustrated by differences in the outlines of migrated cells (Supplementary Fig. 5(a)–(c)).† In softer scaffolds, cells migrated in a wide sheet spanning from one end of the scaffold to the other (Supplementary Fig. 5(a)),† while in the stiffer scaffold, the cells formed slender, tube-like structures (Supplementary Fig. 5(c)).† In an attempt to quantitatively describe the structural differences of migrated cells, normalized area is plotted against normalized length (Supplementary Fig. 6).† The data from stiffer gels (pH 11) lie below the data from softer gels (pH 7.4) with smaller [Sn]. The difference is quite apparent and provides an automated means to distinguish experiments in which true capillaries are formed from those in which the cells migrate in a sheet along the gel-coverslip interface. This observation implies the existence of different modes of cell migration in scaffolds with different stiffness and therefore raises the prospect of controlling cell migration behavior by varying the mechanical properties of the scaffold.

Endothelial cell migration under co-culture conditions.

A major advantage of this new design is its capability to study cell migration through 3D matrices and across endothelial layers under co-culture conditions. Cancer cell intravasation has previously been shown to be a process in which cancer cells interact with and penetrate through the endothelial monolayer.[36,37] It is also well established that cancer stromal cells signal to endothelial cells for angiogenesis.[38,39,44] In cancer therapy, impeding angiogenesis is critical along with chemotherapy and other treatments.[38] These interactions can be investigated in our microfluidic platform by co-culturing endothelial cells with various types of cancer cell. MTLn3 or U87MG were cultured in

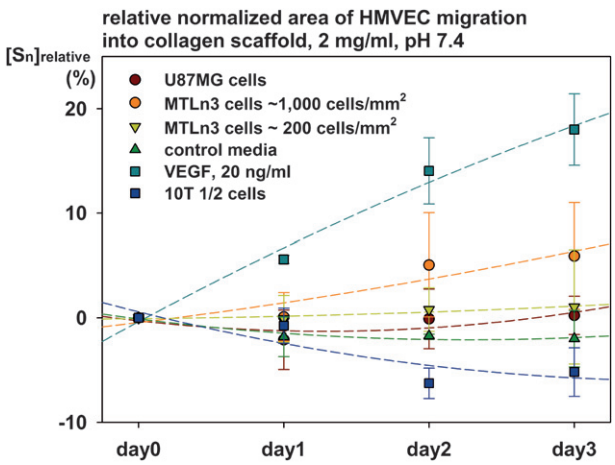

Fig. 5 Migration of HMVEC cells in response to signals from other cell types (U87MG, MTLn3, 10T 1/2) in combination with a VEGF gradient. Change of relative normalized area of HMVEC cultured in the cell channel, with different cell types in the condition channel (U87MG cells, MTLn3 cells with different seeding density and 10T 1/2 cells), only control media without cells (control media), and control media with 20 ng/ml VEGF (VEGF, 20 ng/ml). VEGF containing medium and MTLn3 cells seeded at high density attracted HMVEC strongly, while low density MTLn3 cells and U87MG cells did not. With 10T 1/2 cells in the condition channel, HMVEC tended to migrate to the control side. Each point represents an average with $n = 8$ (8 scaffolds; 4 devices) for each condition. Error bars represent standard deviation.

the condition channel and HMVEC were cultured in the cell channel. In our preliminary observations, high density MTLn3 attracted HMVEC into the collagen scaffold (Fig. 4(a)), but the migration rate was significantly slowed compared to that observed with a VEGF gradient (20 ng/ml in condition channel) (Fig. 5), suggesting that the chemical factors generated by MTLn3 cells are less stimulatory than 20 ng/ml VEGF gradient. Low density MTLn3 cells did not induce significant migration of HMVEC. This result is likely due to the greater concentrations of secreted factors generated by the higher cell concentration, but could also be due to depletion of oxygen and nutrients from the medium by the higher MTLn3 cell density. U87MG cells appeared not to attract HMVEC, in spite of high cell density in the condition channel (Fig. 4(b)). Compared to MTLn3 cells, U87MG cells showed faster migration into the scaffolds.

The communication between vascular smooth muscle cells (10T 1/2) and endothelial cells were also studied by seeding 10T 1/2 cells in the condition channel and HMVEC in the cell channel. These two cell types likely communicate with each other during the process of vascular growth and remodeling. 10T 1/2 cells were found to exert a stabilizing influence on HMVEC. Migration of HMVEC was suppressed on both sides of the cell channel, but sometimes they migrated only on the control side leaving the condition side stable (Fig. 4(c)). This can also be seen from the quantitative measures described above (Fig. 5). Further experiments using this co-culture strategy could be used to investigate the role of 10T 1/2 recruitment to endothelial cells in stabilizing newly formed capillaries as has been suggested in previous works.[40–43]

Conclusion

This novel microfluidic platform has proven to be a versatile and powerful tool to study cell migration for various biological applications. It provides a well-controlled cell culture environment which can be observed in real time. Furthermore, it allows for an integration of biophysical and biochemical factors, essential in mimicking physiological conditions as cells constantly receive signals from both their soluble and insoluble environments. We are now exploring new applications with this platform as a model system for physiological and pathophysiological phenomena such as angiogenesis, arteriogenesis, cancer intravasation and extravasation[43] by introducing cells at different time points, different densities and different seeding arrangements.

Acknowledgements

We would like to thank Tharathorn Rimchala, Douglas Lauffenburger and Frank Gertler for valuable discussions and for providing the cancer cells (MTLn3, U87MG), Guillermo Garcia-Cardena for kindly providing the smooth muscle cells (10T 1/2) and Jose Antonio Sanz-Hererrea for analyzing the diffusion experiments. The research is supported by the National Science Foundation (EFRI-0735997) and IR&D Project N. DL-H-550151, Draper Laboratories Inc.

References

1 H. Gerhardt, M. Golding, M. Fruttiger, C. Ruhrberg, A. Lundkvist, A. Abramsson, M. Jeltsch, C. Mitchell, K. Alitalo, D. Shima and C. Betsholtz, *J Cell Biol*, 2003, **161**, 1163.
2 C.-L. Helm, M. Fleury, A. Zisch, F. Boschetti and M. Swartz, *Proc Natl Acad Sci USA*, 2005, **102**, 15779.
3 M. Zaman, L. Trapani, A. Sieminski, D. MacKellar, H. Gong, R. Kamm, A. Wells, D. Lauffenburger and P. Matsudaira, *Proc Natl Acad Sci USA*, 2006, **103**, 10889.
4 A. Sieminski, R. Hebbel and K. Gooch, *Exp Cell Res*, 2004, **297**, 574.
5 N. Yamamura, R. Sudo, M. Ikeda and K. Tanishita, *Tissue Eng*, 2007, **13**, 1443.
6 R. Jain, K. Schlenger, M. Hockel and F. Yuan, *Nat Med*, 1997, **3**, 1203.
7 K. Nakayasu, N. Hayashi, S. Okisaka and N. Sato, *Invest Ophth Vis Sci*, 1992, **33**, 3050.
8 Y. Shiu, J. Weiss, J. Hoying, M. Iwamoto, I. Joung and C. Quam, *Crit Rev Biomed Eng*, 2005, **33**, 431.
9 G. Davis, S. Black and K. Bayless, *In Vitro Cell Dev Biol–Anim*, 2000, **36**, 513.
10 P. DiMilla, J. Quinn, S. Albeida and D. Lauffenburger, *AIChe J*, 1992, **38**, 1092.
11 Y. Shizukuda, A. Helisch, R. Yokota and J. Anthony Ware, *Circ Res*, 1999, **84**, 247.
12 J. Rojas, S. Sennoune, D. Malti, K. Bakunts, M. Reuveni, S. Sanka, G. Martinez, E. Seftor, C. Meininger, G. Wu, D. Wesson, M. Hendrix and R. Martinez-Zaguilan, *Am J Physiol Heart Circ Physiol*, 2006, **291**, H1147.
13 S. Sagnella, F. Kligman, E. Anderson, J. King, G. Murugesan, R. Marchant and K. Kottke-Marchant, *Biomaterials*, 2004, **25**, 1249.
14 M. Hendrix, E. Seftor, R. Seftor and I. Fidler, *Cancer Lett*, 1987, **38**, 137.
15 K. Mace, S. Hansen, C. Myers, D. Young and N. Boudreau, *J Cell Sci*, 2005, **118**, 2567.
16 S. Even-Ram and K. M. Yamada, *Current Opinion in Cell Biology*, 2005, **17**(5), 524.
17 K. Bayless, R. Salazar and G. Davis, *Am J Pathol*, 2000, **156**, 1673.
18 A. Wenger, A. Stahl, H. Weber, G. Finkenzeller, H. Augustin, G. Stark and U. Kneser, *Tissue Eng*, 2004, **10**, 1536.
19 C. Ghajar, K. Blevins, C. Hughes, S. George and A. Putnam, *Tissue Eng*, 2006, **12**, 2875.
20 M. Chicurel, *Science*, 2002, **295**, 606.
21 D. Selmeczi, S. Mosier, P. Hagedom, N. Larsen and H. Flyvbjerg, *Biophys. J*, 2005, **89**, 912.
22 N. Jeon, H. Baskaran, S. Dertinger, G. Whitesides, L. Van De Water and M. Toner, *Nat Biotechnol*, 2002, **20**, 826.
23 B. Chung, L. Flanagan, S. Rhee, P. Schwarz, A. Lee, E. Monuki and N. Jeon, *Lab Chip*, 2005, **5**, 401.
24 A. Tourovskaia, X. Figueroa-Masot and A. Folch, *Lab Chip*, 2005, **5**, 14.
25 R. Gomez-Sjoberg, A. Leyrat, D. Pirone, C. Chen and S. Quake, *Anal Chem*, 2007, **79**, 8557.
26 W. Gu, X. Zhu, N. Futai, B. Cho and S. Takayama, *Proc Natl Acad Sci USA*, 2004, **101**, 15861.
27 T. Frisk, S. Rydholm, T. Liebmann, H. Svahn, G. Stemme and H. Brismar, *Electrophoresis*, 2007, **28**, 4705.
28 W. Saadi, S. Rhee, F. Lin, B. Vahidi, B. Chung and N. Jeon, *Biomed Microdevices*, 2007, **9**, 627.
29 V. Vickerman, J. Blundo, S. Chung and R. Kamm, *Lab Chip*, 2008, **8**, 1468, DOI: 10.1039/b802395f.
30 S. Y. Cheng, S. Heilman, M. Wasserman, S. Archer, M. L. Shuler and M. Wu, *Lab Chip*, 2007, **7**, 763.
31 A. Paguirigan and D. Beebe, *Lab Chip*, 2006, **6**, 407.
32 G. Yancopoulos, S. Davis, N. Gale, J. Rudge, S. Wiegand and J. Holash, *Nature*, 2000, **407**, 242.
33 L. Coultas, K. Chawengsaksophak and J. Rossant, *Nature*, 2005, **438**, 937.
34 G. Walker and D. Beebe, *Lab Chip*, 2002, **2**, 131.
35 U. Cavallaro, S. Liebner and E. Dejana, *Exp Cell Res*, 2006, **312**, 659.
36 P. Carmeliet and R. Jain, *Nature*, 2000, **407**, 249.
37 P. Carmeliet, *Nature*, 2005, **438**, 932.
38 N. Ferrara and R. Kerbel, *Nature*, 2005, **438**, 967.
39 J. Folkman, *Nature Reviews*, 2007, **6**, 273.
40 R. Montesano, L. Orci and P. Vassalli, *J Cell Biol*, 1983, **97**, 1648.
41 Y. Zhao, Y. Tan, L. Zhou, H. Wang and Y. Mao, *Stroke*, 2007, **38**, 1313.
42 P. Carmeliet, *Nat Med*, 2000, **6**, 389.
43 G. Gerthoffer, *Circ Res*, 2007, **100**, 607.
44 S. Suresh, *Acta Biomater*, 2007, **3**, 413.